Reference Modulation for Calibrated Measurements of Tag Backscatter

Daniel G. Kuester*†, David R. Novotny*, Jeffrey R. Guerrieri*, Randal Direen*, and Zoya Popović†

* U.S. Department of Commerce, National Institute of Standards and Technology, Boulder, CO, USA 80304
{daniel.kuester, david.novotny, jeffrey.guerrieri, randy.direen} at nist.gov
† University of Colorado, Department of Electrical, Computer, and Energy Engineering, Boulder, CO, USA 80309
{daniel.kuester, zoya.popovic} at colorado.edu

***Abstract*—We present a model and reference backscatter device for calibrating measurements of 860-960 MHz Ultra-High Frequency (UHF) tag backscattering. The model relates transmission to and backscattering from the device with a modulation depth calculable from circuit parameters. Unlike the free-space far field approximations, the model is valid in arbitrary stationary linear environments, including the near field of a transmit or measurement antenna, via *S*-parameters. We use the model to demonstrate an inexpensive reference backscatter device with a common lab switch and loads. Validation measurements on a network analyzer with two expressions for modulation depth agree to within 0.1 dB at 915 MHz. Finally, we present some initial calibrated measurements of backscattered power from a tag at 915 MHz, with estimated uncertainty -0.7 dB to +0.6 dB.**

I. Introduction

Radio frequency identification (RFID) deployments are continuing to proliferate in various worldwide bands within 860-960 MHz [1]. Passive transponders ("tags") require less and less power from transceivers ("readers") to turn on, which allows larger operation range but requiring readers to detect fainter and fainter tag replies. This suggests a risk that existing interference problems [3] will get worse, and that reader detection of tags may become a dominant constraint on practical communication [2]. Unfortunately, standardized backscatter performance tests are immature for tags, and do not yet exist for readers.

Operation of readers and tags are more tightly standardized than performance tests. Most passive commercial systems comply with the EPC Global "UHF Class 1 Gen 2" and ISO 18000-6 standards, which outline the operation and parameters of the half-duplex protocol used by RFID in these bands. In the forward link, a reader transmits a modulated carrier toward a tag field, which uses the incident energy as a power supply. The tags reply by time-varying their antenna load impedances, which encodes information in slight variations in the carrier reflection received at a reader. This modulated backscattering approach, known as load modulation, forms the return link. Similar processes have been used for antenna measurements [4] and espionage [5].

Test standards, in contrast, still have gaps to be addressed, especially in the return link. They do not yet address reader sensitivity or interference rejection, though and suggest that reader sensitivity is becoming an increasingly important system range constraint [2] and readers are more vulnerable to interference than tags [3]. Standard ISO 18047-6 [6] outlines tests for tag backscattering performance defined as the difference between the radar cross section values in its two load modulation states. The test method calibrates tag backscattering by measuring the change in reflected power caused by introducing a shorted dipole standard into the test environment.

This calibration has drawbacks. One author estimated the measurement uncertainty of this method at approximately 2 dB [7]. In addition to errors in this estimate, the current ISO 18047-6 method neglects phase effects by directly adding and subtracting power quantities, even though existing work [8][9] explains accounting for phase. Adding and remov-

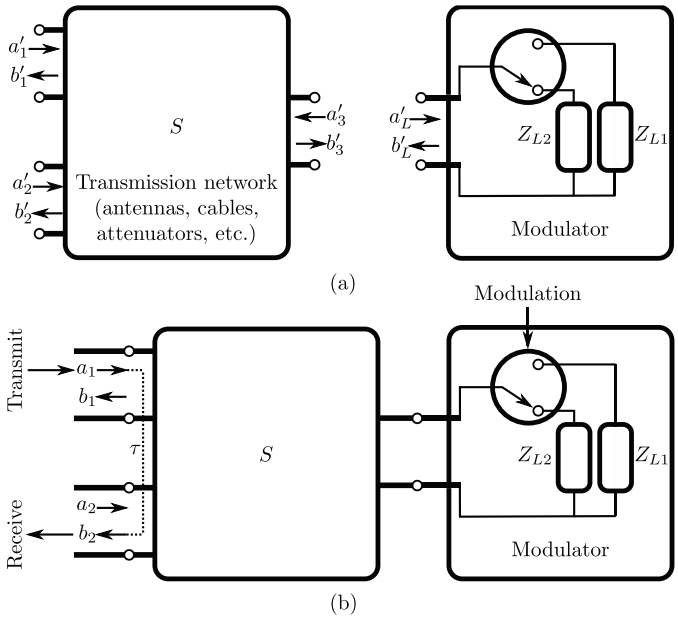

Fig. 1. Reference backscattering model illustrating S-parameters with the modulator (a) disconnected and (b) connected to the transmission network. When connected, a transmitter delivers a traveling wave a_1 into port 1 of an arbitrary transmission system S, which is described in (a). The reflection coefficient presented to waves arriving at port 3 switches between $\Gamma_L \rightarrow \Gamma_{L1}$ (the Z_{L1} state) and $\Gamma_L \rightarrow \Gamma_{L2}$ (the Z_{L2} state). Reflection back to port 2 is the traveling wave b_2. The transmit-to-receive transmission coefficient including tag reflections is $\tau = b_2/a_1$.

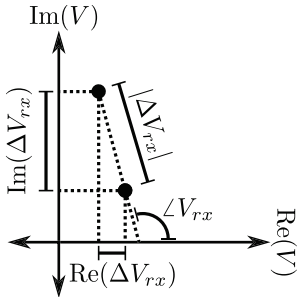

Fig. 2. Illustration of demodulated ΔV_{rx} on the complex (IQ) plane received from a reference backscatterer. The signal is shown in rectangular coordinates as $\mathrm{Re}(\Delta V_{rx}) + j\mathrm{Im}(\Delta V_{rx})$, and polar form as magnitude and phase.

ing the entire shorted dipole standard adds structural-mode modulation to the calibration signal, which interacts with environmental scattering differently [2] from the antenna-mode modulation [8][9] of actual tags. As a result of these factors, measurements may not be repeatable between different test setups and test environments.

To work toward addressing these shortcomings, we offer here a new model and backscattering standard for more accurate signal level calibrations of tag backscattering across 860-960 MHz. Our linear network model uses S-parameters to describe backscattering in the system illustrated in Fig. 1. It is composed of a two-port transceiver, a one-port modulator load, and a three-port linear network representing the unknown environment between them. Though the switching in the modulator makes it nonlinear, we use traveling-wave S-parameters under the assumption that the device is linear in each state. We develop the model to show how transmission and backscattering are related by modulator circuit parameters in arbitrary environments.

We then realize a backscatter reference standard, with a diode switch in place of the ideal switch in the model. The switch loads are a short and a matched 50 Ω measurement instrument serving as the matched modulation load and to measure transmitted waves from a reader. With some calibration measurements of circuit parameters of the switch and the backscattering antenna, and measurements of transmission from the reader, it is possible to predict the "correct" signal measured on our spectrum analyzer with less uncertainty than the instrument. We calibrate a tag under test's measured backscatter signal with the reference backscatter signal for traceable and more accurate measurements of tag backscatter. As an initial example of this measurement approach, we give a calibrated tag backscatter measurement swept against power at 915 MHz.

II. Link and load modulation model

Our model for transmission and backscattering between a transmitter, load-modulated backscatterer, and receiver is illustrated in Fig. 1. The linear and reciprocal transmission network, which can incorporate any arbitrary cables, antennas, linear propagation effects, and any other linear circuit elements, is shown as S. Transmit and measurement are at ports 1 and 2, and our backscatter modulator will load port 3.

When the two networks are disconnected (Fig. 1a), transmission coefficients between the loaded ports in the reciprocal transmission environment are $S_{23} = S_{32} = b'_3/a'_2$ and $S_{31} = S_{13} = b'_3/a'_1$. Looking into the transmission network from port 3 is the reflection coefficient $S_{33} = b'_3/a'_3$ that will be presented to the modulator. Likewise, the unloaded reflection coefficient into the modulator is $\Gamma_L = b'_L/a'_L$. We can access these coefficients for network analyzer measurements simply by detaching the two network blocks.

When the two networks are connected as shown in Fig. 1b, a carrier into port 1 with switching in the backscatter modulation causes a complex voltage states illustrated in Fig. 2 to appear at port 2. The signal is shown as a phasor V_{rx} switching between two states. We will show here how the modulated signal ΔV_{rx} is related to a transmit signal V_{tx} with circuit parameters of the modulator in arbitrary environments.

The traveling waves a_1 and b_2 in Fig. 1b are $a_1 = V_{tx}/Z_0^{1/2}$ and $b_2 = V_{rx}/Z_0^{1/2}$, with real port impedances Z_0. An expression for the received wave b_2 in this system with port 3 loaded by the tag is [10]

$$b_2 = \left(S_{21} + \frac{S_{31}S_{23}\Gamma_L}{1 - S_{33}\Gamma_L}\right) a_1 + \left(S_{22} + \frac{S_{32}S_{23}\Gamma_L}{1 - S_{33}\Gamma_L}\right) a_2. \tag{1}$$

Port 2 is a receive port, so we assume there is no output ($a_2 = 0$), a transmission coefficient $\tau = b_2/a_1$ between the transmit and receive ports is

$$\tau = S_{21} + \frac{S_{31}S_{23}\Gamma_L}{1 - S_{33}\Gamma_L}, \tag{2}$$

similar to published two-port models [11]. If the modulator load alternates between $\{Z_{L1}, Z_{L2}\}$ corresponding to reflection coefficients $\Gamma_L \rightarrow \{\Gamma_{L1}, \Gamma_{L2}\}$, then the change in the transmission coefficient $\Delta\tau$ will be

$$\Delta\tau = \frac{\Delta V_{rx}}{V_{tx}} = S_{31}S_{23}\frac{\Gamma_{L2} - \Gamma_{L1}}{(1 - S_{33}\Gamma_{L2})(1 - S_{33}\Gamma_{L1})}. \tag{3}$$

The term on the right offers a convenient definition for a return modulation depth

$$M = \frac{\Gamma_{L2} - \Gamma_{L1}}{(1 - S_{33}\Gamma_{L2})(1 - S_{33}\Gamma_{L1})} = \frac{\Delta\tau}{S_{31}S_{23}} \tag{4}$$

which relates system behavior when the transmission and modulation networks are connected (S_{31} and S_{23}) with measurable parameters from each block separately (Γ_{L1}, Γ_{L2}, and S_{33}).

The relationship expressed in terms of received modulation power P_{rx} between the two switched states at the reader, transmission link losses $|S_{31}|^2$ and $|S_{23}|^2$, and the continuous-wave transmit power P_{tx} is

$$\frac{P_{rx}}{P_{tx}} = \frac{|\Delta V_{rx}|^2/Z_0}{|V_{tx}|^2/Z_0} = |\Delta\tau|^2 = |S_{31}|^2|S_{23}|^2|M|^2. \tag{5}$$

This relationship applies most visibly to bistatic measurement antenna configurations, with antennas and cables looking into ports 1 and 2 of Fig. 1. It also applies to monostatic configurations, if we model a lossless circulator inside the transmission network S between an antenna and ports 1 and 2.

To relate this result with free space models, consider an idealized monostatic system in an anechoic environment. The backscattering and detection antennas are well-matched and copolarized, and we will assume there are no near-field effects. Measurement and backscattering antennas are oriented with gains G and G_{bs}. If a low-loss circulator is used to separate the transmit and receive channels, then the received modulated power can be estimated with the well-known Friis transmission equation in place of $|S_{31}|^2 = |S_{23}|^2$ in (5) so that

$$\frac{P_{rx}}{P_{tx}} = G^2 G_{bs}^2 \left(\frac{\lambda}{4\pi R}\right)^4 |M|^2 \tag{6}$$

where R is the range between the measurement and backscattering antennas and λ is the free-space carrier wavelength. This makes the same assumptions as the radar equation, and has the same form, so we can tie it to the modulated radar cross section σ_{mod} (see for example [1]) used for tags:

$$\sigma_{mod} = \frac{G_{bs}^2 \lambda^2 |M|^2}{4\pi}. \tag{7}$$

Now the model is developed enough to use in calibrations of received backscatter measurements, so we will move on to implementation.

III. Reference backscatter calibrations

A. Calibrated signal generation

We built a modulator shown in Fig. 3 to realize the modulator model in Fig. 1. Connecting a network analyzer or power meter as Z_{L2} serves as a matched modulation state $|\Gamma_{L2}| \approx 0$ and allows us to measure transmission from the tag interrogation to the modulator. The other modulation state is a short, so $|\Gamma_{L1}| \approx 1$. Because we expect $|\Gamma_{L2} - \Gamma_{L1}|$ to be approximately 1, and the backscatter antenna is matched, giving it small $|S_{33}|$, we expect M to be near 0 dB. We chose a switch with nominal 20 ns switching time to within 10% of steady state, which is much faster than the 640 kHz symbol maximum symbol rate for tags compliant with ISO 18000-6C.

The modulated power received by the spectrum analyzer from the reference backscatter can be determined in three broad steps:

1) Calibrate M: Calibrate $|M|$ in advance by measuring the terms in equation (4) with a network analyzer. We will show during validation that measurements can be performed with either expression in this equation.

One advantage of measuring Γ_{L2}, Γ_{L1}, and S_{33} directly is that (to first order) measurement dynamic range is not changed by moving the antenna attached to the reference modulator, especially in an anechoic environment. Another is that Γ_{L2} and Γ_{L1} can be measured with phase-stable cables near the network analyzer for a accurate measurements. This choice of measurements only needs one antenna (for the modulator), so the connection between antennas and transmitters and measurement equipment does not need to be broken.

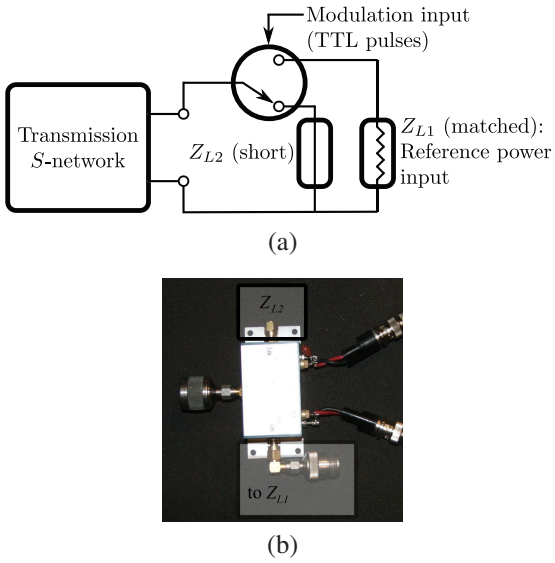

Fig. 3. Block diagram (a) and realization (b) of a modulation switch for reference backscatter calibrations. The load Z_{L1} is intended to connect with a matched 50 Ω instrument such as a power sensor or network analyzer, to measure power delivered to the backscatter reference and serve as a modulation state. This realization is shown with ±5 V DC biasing inputs.

Calibrating M with measurements of $\Delta\tau$ and measurements of propagation losses S_{23} and S_{31} has different advantages. Transmission measurements of propagation losses can have smaller uncertainties than the reflection measurements in the first approach, if cables are kept stable. It also needs fewer measurements, which may reduce the contribution of mistakes to measurement error.

More work needs to be done understanding the uncertainties in these approaches, which we hope to address in future work.

2) Power measurements of transmission: Next, we need to measure $|S_{31}|^2$ and $|S_{23}|^2 = |S_{32}|^2$ with power meter measurements of transmit power from each interrogator port and power received at the reference modulator. We used a real switch with insertion losses, so we de-embed the effect of the switch losses to the interface between the switch and the antenna via transfer (T) parameters.

3) Calculate reference backscatter power: Finally, we can calculate the reference backscattered power $P_{rx}^{(ref)}$ with the previous measurements and equation (5).

B. Validation

To validate reference modulation, we measured backscatter excited from the modulator with an interrogation signal at 915 MHz. Signals measured from the scatter modulator with 20 kHz square pulse inputs are shown measured with a spectrum analyzer Fig. 4. The sidebands are consistent with the square modulation realized with the switch and the pulse generator.

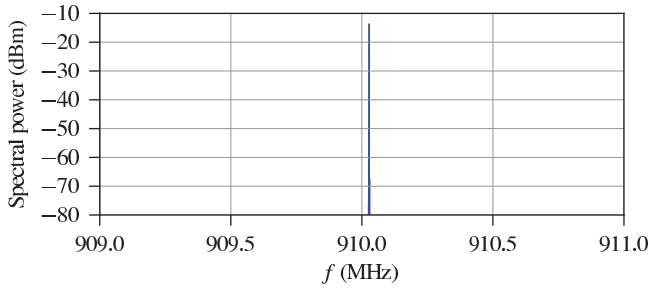

(a)

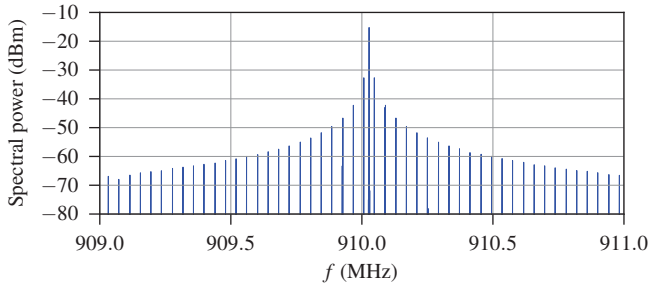

(b)

Fig. 4. Spectrum analyzer traces of (a) unmodulated carrier leakage into the receive antenna, then (b) load-modulated at 20 kHz with the device in Fig. 3. In both cases, the signal generator transmitted the carrier at 12.1 dBm to the modulator antenna, placed boresight approximately 50 cm from a pair of transmit and receive antennas with 8 ± 1 dBi gain.

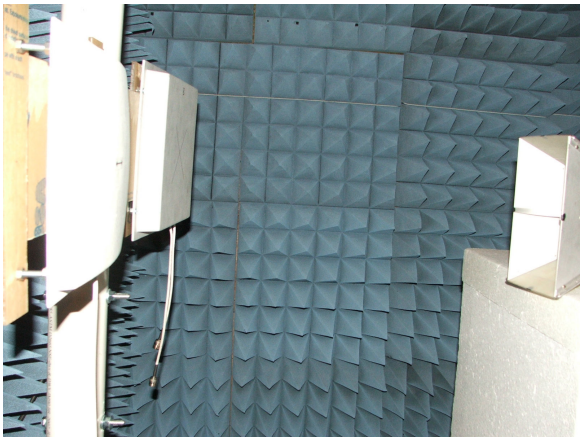

Fig. 5. The antenna transmission network we tested to validate the model in section II, using the horn backscatter reference shown in Fig. 3

We also need to validate the levels for the calibration. The model in equation (4) gives us two expressions for M in terms of transmission and reflection coefficients. We can take advantage of this to validate our model by measuring both expressions with a network analyzer in controlled S transmission networks.

We measured modulation through the anechoic environment pictured in Fig. 5 with the modulator on the standard gain horn on the right serving as our reference backscatter source. The measurement is monostatic (with the antenna shown in the foreground) as discussed in section II (e.g,. assuming

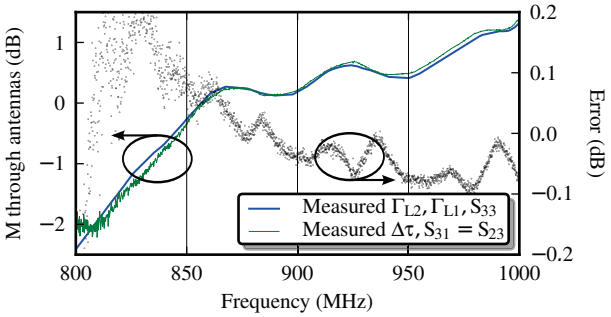

Fig. 6. Validation of the reference backscatter with a network analyzer for antenna transmission shown in Fig. 5, computed with measurements of the terms in (4). The curves agree to ±0.1 dB over the 860-960 MHz tag response bandwidth.

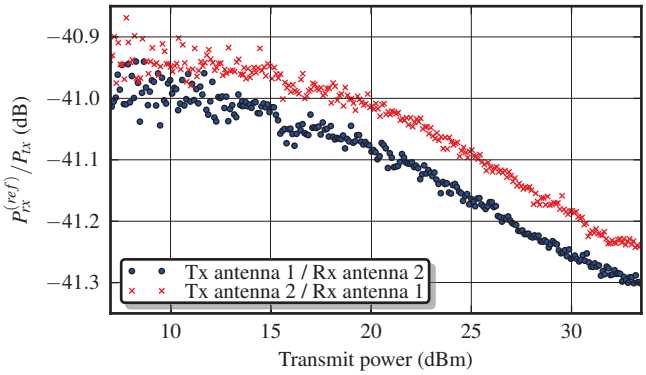

Fig. 7. Reference backscatter linearity tests, measured with the with the bistatic configuration shown in Fig. 5. The backscatter reference load-modulated 915 MHz carrier reflections at 160 kHz with the circuit described in Fig. 3. Reference backscattered power is $|\Delta V_{rx}|^2/(2Z_0)$ from demodulated IQ measured on a spectrum analyzer with 8 MHz analysis bandwidth. Though the traces would be ideally constant (linear) and equal (by antenna reciprocity), there is drift up to 0.3 dB and disagreement as high as 0.12 dB.

ports 1 and 2 lead to two ports of an ideal circulator). The detection antenna is a commercial RFID patch with 10 dB of return loss across 895-940 MHz. In this case, by symmetry, the change in reflection coefficient at into the antenna was taken to be the same as $\Delta\tau$. We use the anechoic environment to reduce interference from outside signals, but stress that the model and calibration works equally well in complex reflective environments.

Results are shown in Fig. 6. Across the 860-960 MHz tag response bandwidth, the two measurements of M agree within 0.1 dB. Below 860 MHz, detection antenna mismatch causes more error by lowering the measurement dynamic range of the transmission measurement in the network analyzer.

A final validation is shown in Fig. 7 for system linearity. This measurement was performed bistatically with both of the antennas on the left of Fig. 5. We give a pair of measurements taken by transmitting from each antenna in Fig. 5, to validate results that should be the same by reciprocity. Results between the two traces agreed to within 0.12 dB, and each trace varied by less than 0.3 dB.

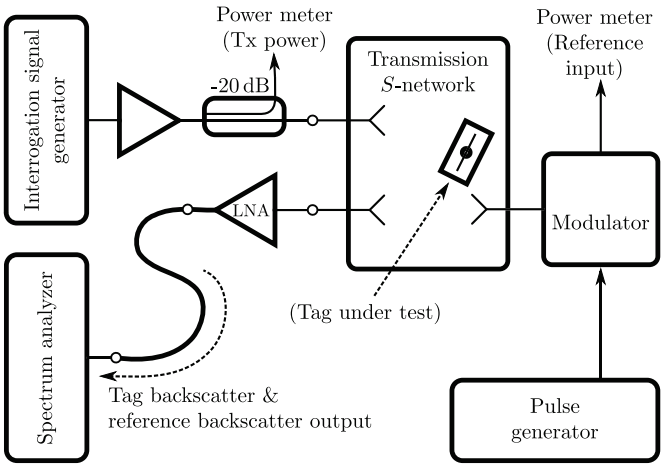

Fig. 8. Setup for calibrated tag backscattering measurements. Measurements were automated by computer with a general purpose interface bus (GPIB) connection.

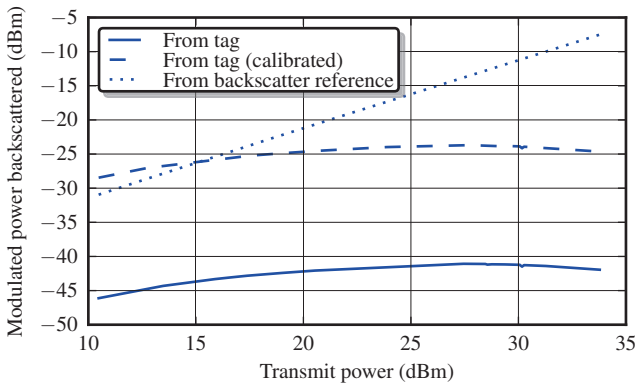

Fig. 9. Measurements of backscattered power comparing raw tag and reference signals with the calibrated measurement of the tag. The reference was switched at 160 kHz modulation, and the tag was interrogated with signal parameters described in table I. Signals from each were measured with IQ demodulation as in Fig. 7. The calibration used M calculated with equation (4) from measurements of Γ_{L1}, Γ_{L2}, and S_{33} .

C. Calibrated tag measurements

With some validation completed, we can now show an example tag backscatter measurement calibrated with the backscattering source. Our overall test setup is summarized in Fig. 8. Instruments were controlled from a computer via general purpose interface bus (GPIB).

The calibrated measurement is shown in Fig. 9, with raw measurements of the tag under test and the reference backscatter. A query command begins the tag transaction with parameters listed in Table I. Reference backscatter was measured during the period after the tag response (while the carrier is left on to power the tag, but the tag is not responding).

Our initial estimate for the calibrated tag backscatter measurement uncertainty, based partly on the validation data shown in Figs. 6 and 7, is shown in Table IIa. For comparison, we also estimate uncertainty in the measurement without a backscattering standard in Table IIb, which is dominated by our spectrum analyzer's demodulated signal measurement uncertainty but with further uncertainty in the path loss between the measurement antenna and the spectrum analyzer. The demodulated measurement is based on the manufacturer's specification for *absolute* measurement uncertainty. This term is smaller for the calibrated measurement result because the instrument is used to compare the tag signal with the reference, which depends on the negligibly small *relative* measurement uncertainty. Finally, Table IIc gives an estimate of the uncertainty of backscattered tag signals calibrated against the thin $\lambda/2$ rod prescribed in ISO 18047-6. Because thin rods are not common standards for RCS calibrations, more work is necessary to estimate uncertainty of this measurement.

Reader-to-tag modulation	PR-ASK
Tag-to-reader modulation	FM0
Tag-to-reader link rate (BLF)	160 kHz
Reader-to-tag link rate	160 kHz (data 0) 91 kHz (data 1)
Anticollision slots (Q)	0 (no slots)
Delay after tag response† (T2)	11.7 µs
Tari	6.25 µs

† Reference backscattering was measured during this period

TABLE I
ISO/IEC 18000-6C TAG QUERY PARAMETERS

Backscattered tag signal measurement (with reference backscatter calibration)

M calibration	±0.3 dB
Power measurements	±0.05 dB
Nonlinearity	±0.3 dB
Total	−0.7 dB, +0.6 dB

(a)

Backscattered tag signal measurement (with spectrum analyzer alignment only)

Power measurements	±0.05 dB
Measurement cable losses	±0.15 dB
Instrument uncertainty	±0.9 dB
Total	−1.2 dB, +1.1 dB

(b)

Backscattered tag signal measurement (with ISO 18047-6 $\lambda/2$ rod calibration)

Power measurements	±0.05 dB
Measurement cable losses	±0.15 dB
Nonlinearity	±0.3 dB
Multipath	±0.9 dB [2]
$\lambda/2$ rod RCS uncertainty	(unknown)
Total	−1.5 dB, +1.3 dB (without rod RCS uncertainty)

(c)

TABLE II
MEASUREMENT UNCERTAINTY ESTIMATES, k=2

IV. CONCLUSION

The calibration approach we showed here is for signal levels and not fields. In the future, we wish to extend this work to simplify test methods based on network theory, as discussed in [9]. Reference backscatter generated with a

reference antenna with known gain could, however, be used to generate a calibrated modulated radar cross section reference with equation (7).

We are also interested in extending this reference backscattering method to calibrated tests of reader sensitivity and interference performance.

V. Acknowledgements

The United States Department of Homeland Security Science and Technology Directorate has, in part, sponsored the production of this material with NIST. The authors also appreciate Ed Kuester's helpful analysis guidance.

References

[1] D.M. Dobkin, *The RF in RFID: Passive UHF RFID in Practice*, Newton, MA, USA: Newnes, 2007, pp. 19-22.

[2] D.G. Kuester, D.R. Novotny, J.R. Guerrieri, "The relative importance of the forward and reverse links in propagating UHF RFID with passive tags," *Proc. 2010 IEEE Symp. on Electromagnetic Compatibility*, pp. 680-685.

[3] M.R. Souryal, D.R. Novotny, D.G. Kuester, J.R. Guerrieri, K.A. Remley, "Impact of RF Interference between a Passive RFID System and a Frequency Hopping Communications System in the 900 MHz ISM Band," *Proc. 2010 IEEE Symp. on Electromagnetic Compatibility*, pp. 495-501.

[4] J.H. Richmond, "A Modulated Scattering Technique for Measurement of Field Distributions," *IRE Trans. on Microwave Theory and Techniques*, vol.3, no.4, pp. 13-15, July 1955.

[5] A. Glinsky, *Theremin: Ether Music and Espionage*." Champaign, IL, USA: University of Illinois Press, 2000, pp. 259-273.

[6] *Radio frequency identification device conformance test methods — Test methods for air interface communications at 860 MHz to 960 MHz*, ISO/IEC standard 18047-6, 2006.

[7] A. Pouzin, T.P. Vuong, S. Tedjini, M. Pouyet, J. Perdereau, and L. Dreux, "Determination of measurement uncertainties applied to the RCS and the differential RCS of UHF passive RFID tags," *Proc. Antennas and Propagation Soc. Int. Symp., 2009*, pp. 1-4.

[8] P. Nikitin and K. Rao, "Theory and measurement of backscattering from RFID tags," *IEEE Antennas and Propagation Magazine*, vol. 48, 2006, p. 212–218.

[9] P.V. Nikitin and K.V.S. Rao, "Effect of Gen2 Protocol Parameters on RFID Tag Performance," *Proc. 2009 Intl. Conf. on RFID*, pp. 117-122, 28-29 Apr. 2009.

[10] D.M. Kerns, R.W. Beatty, *Basic Theory of Waveguide Junctions and Introductory Microwave Network Analysis*. Oxford: Pergamon Press, 1967, p. 108.

[11] K. Seemann, F. Cilek, M. Schmidt, R. Weigel, "RFID at UHF Frequencies: The Passive Transponder Frontend Approach," *Proc. Intl. Conf. on Microwaves, Radar & Wireless Communications, 2006*, pp.657-661, 22-24 May 2006.